Available online at http://scik.org

J. Math. Comput. Sci. 11 (2021), No. 6, 7154-7169

https://doi.org/10.28919/jmcs/6149

ISSN: 1927-5307

HEAT SOURCE AND RADIATION ABSORPTION ON UNSTEADY MHD FLUID FLOW OVER AN INFINITE VERTICAL PLATE EMBEDDED IN A POROUS MEDIUM IN PRESENCE OF SORET EFFECT

BIJOY KRISHNA TAID*, NAZIBUDDIN AHMED, SUBHRAJIT SARMA

Department of Mathematics, Gauhati University, Guwahati-781014, India

Abstract: In this paper, an investigation on the heat source and radiation absorption on MHD fluid flow past an accelerated vertical plate embedded in a porous medium with variable thermal diffusion are carried out. The dimensionless governing equations are solved using closed form of Laplace transformation technique. The velocity, temperature, concentration profiles, Nusselt number and Sherwood number are graphically interpreted to various physical parameters like thermal Grashof number, time, Accelerating parameter, Prandtl number and Permeability parameter, Magnetic parameter, Schmidt number, Mass Grashof number and Soret number etc. It has been found that velocity, concentration and Nusselt number rise with the increasing Prandtl number. Further, temperature and Sherwood number decreases with increment in Prandtl number.

Keywords: MHD; heat source; Porous medium; Soret effect; Laplace transform.

2010 AMS Subject Classification: 44A10.

*Corresponding author

E-mail address: bijoytaid@gmail.com

Received May 27, 2021

1. INTRODUCTION

Magnetohydrodynamics principle finds numerous applications in astrophysics, missile technology, plasma physics, space technology and cosmology. The application of MHD concepts can be seen in medical and biological research on a regular basis. Several prominent writers, including Alfven [1], Shercliff [2], Ferraro and Plumpton [3], and Crammer and Pai [4], contributed to the development of MHD in its current form. In recent years, the flow of fluids through porous media have been of principal interest because these are quite prevalent in nature. Due to their application in many branches of science and technology, such flows have piqued the interest of a number of scholars. They facilitate in the study of natural gas, oil, and water movement across oil reservoirs in petroleum technology. Nield and Bejan [5] provided a thorough overview of the studies of convective heat transfer mechanisms via porous media. The effect of free convection on oscillatory flow through a porous medium was studied by Hiremath and Patil [6]. Thermal radiation is studied numerically with various effects by Rao et al. [7], Mahato et al. [8], Ekakitie et al. [9], Lavanya et al [10]. Chemical reactions and thermal radiation effects on unstable blood flow through a parallel and horizontal plate in a porous medium were investigated by Omamoke et al. [11]. The effect of radiation on MHD mixed convection flow around a vertical plate was analyzed by Orhan and Ahmet [12]. Sandeep [13] investigated the effects of radiation and inclined magnetic fields on unsteady hydromagnetic free convection flow in a porous medium past an impulsively moving vertical plate.

The heat transfer phenomenon is crucial in a variety of industrial and environmental problems. Production and conversion of electrical power generation, electricity, maximization of heat transfer rates for preserving the integrity of materials in high temperature environments and cryogenics are all examples of industrial problems. The heat transfer theory is also applicable to human physiology research. Sharma et al. [14] addressed fluctuating heat and mass transfer on 3D flow through a porous medium. The effect of radiation and mass transfer on MHD free convection flow through porous medium was studied by Pattnaik et al. [15]. Selvaraj and Jothi [16] investigated the effect of heat on MHD and radiation absorption fluid flow past a vertical plate with variable temperature and mass diffusion through porous medium. Rajesh and Varma [17] investigated the effects of a heat source on MHD flow through a porous medium past an exponentially accelerated vertical plate with variable temperature. MHD natural convection flow with radiative heat transfer past an impulsively moving plate with ramped wall temperature was studied by Seth et al. [18]. Raju et al. [19] addressed the effects of heat absorption and thermal radiation on an unsteady MHD free convective fluid flow over an infinite vertical plate embedded in porous medium in the presence of Soret and Dufour effects. The effect of radiation and Soret on transient MHD force convection from an impulsively started infinite vertical plate was discussed by Ahmed [20]. The Soret and Dufour effects on mixed MHD convection flow past an infinite vertical porous plate with thermal radiation were examined by Ahmed and Sengupta [21]. Ahmed [22] determined that MHD convection with diffusion-thermo and thermal-diffusion effects in 3D flow past an infinite vertical porous plate.

2. Mathematical Formulation

Consider the transitory movement of an infinite vertical plate through a porous medium past an electrically conductive viscous fluid with varying temperature. The constant asset B_0 a virtual to the plate is intended to be used inversely to the plate. Since the hypnotic Reynolds value of movement is so small so the induced hypnotic region is ignored. The X-axis is taken upwards through vertical plate and y-axis is taken normal to the applied aligned magnetic field. Initially, the liquid as well as the plate are at the same temperature T_∞ at all points with the same concentration level C_∞. The plate accelerates exponentially with a velocity of $u' = u_0 \exp(a't')$ when t' >0. The plate temperature is linear and high among its peers at its particular level. To plate, time period t' is also combined. The focus in the vicinity is elevated to C_w. The effect of thick scattering is thought to be slight. The instable movement is overlooked in the equations below, according to the steady Boussinesq's calculation.

$$\frac{\partial u'}{\partial t'} = -\frac{\sigma B_0 u'}{\rho} + g\beta\left(T - T_\infty\right) + g\beta_c\left(C - C_\infty\right) + \nu\frac{\partial^2 u'}{\partial y'^2} - \frac{\nu u'}{K^*} \tag{1.1}$$

$$\rho C_p \frac{\partial T}{\partial t'} = \kappa \frac{\partial^2 T}{\partial y'^2} \tag{1.2}$$

$$\frac{\partial C}{\partial t'} = D_M \frac{\partial^2 C}{\partial y'^2} + D_T \frac{\partial^2 T}{\partial y'^2} \tag{1.3}$$

The relevant boundary conditions

$$t' \le 0; \quad u' = 0, T = T_\infty, C = C_\infty \qquad for\ all \quad y' < 0 \tag{2.1}$$

$$t' > 0; \quad u' = v_0 e^{a't'},\ T = T_\infty + \left(T_w - T_\infty\right) e^{a't'},\ C = C_\infty + \left(C_w - C_\infty\right) e^{a't'} \quad at \quad y' = 0 \tag{2.2}$$

$$u' \to 0,\ T \to T_\infty,\ C \to C_\infty \quad as \quad y' \to \infty \tag{2.3}$$

Introducing non-dimensional parameters

$$u = \frac{u'}{v_0},\ t = \frac{t' v_0^{\,2}}{\nu},\ y = \frac{y' v_0}{\nu},\ Gr = \frac{g\beta\nu\left(T_w - T_\infty\right)}{v_0^{\,3}},\ Gc = \frac{g\beta_c \nu\left(C_w - C_\infty\right)}{v_0^{\,3}},$$

$$\theta = \frac{T - T_\infty}{T_w - T_\infty},\ \phi = \frac{C - C_\infty}{C_w - C_\infty},\ M = \frac{\sigma B_0^{\,2}\nu}{\rho v_0^{\,2}},\ \Pr = \frac{\mu C_p}{\kappa},\ Sc = \frac{\nu}{D_M},\ a = \frac{a'\nu}{v_0^{\,2}},$$

$$K = \frac{v_0^{\,2} K^*}{\nu^2},\ Sr = \frac{D_T\left(T_w - T_\infty\right)}{\nu\left(C_w - C_\infty\right)} \tag{3.1}$$

Equations (1.1) - (2.3) lead to

$$\frac{\partial u}{\partial t} = Gr\theta + Gc\phi + \frac{\partial^2 u}{\partial y^2} - Mu - \frac{u}{K} \tag{4.1}$$

$$\frac{\partial \theta}{\partial t} = \frac{1}{\Pr}\frac{\partial^2 \theta}{\partial y^2} \tag{4.2}$$

$$\frac{\partial \phi}{\partial t} = \frac{1}{Sc}\frac{\partial^2 \phi}{\partial y^2} + Sr\frac{\partial^2 \theta}{\partial y^2} \tag{4.3}$$

With boundary conditions

$$t \le 0; \quad u = 0, \theta = 0, \phi = 0 \qquad for\ all\ y < 0 \tag{5.1}$$

$$t > 0; \quad u = e^{at}, \theta = e^{at}, \phi = e^{at} \qquad at \quad y = 0 \tag{5.2}$$

$$u \to 0, \theta \to 0, \phi \to 0 \qquad as\ y \to \infty \tag{5.3}$$

3. METHOD OF SOLUTION

Governing equations (4.1), (4.2) and (4.3) are subjected to Laplace transformations. This transforms the partial differential equations into ordinary differential equations given by:

$$K\frac{d^2\bar{u}}{dy^2}-\left(MK+sK+1\right)\bar{u}=-K\left\{\frac{Gr}{s-a}e^{-\sqrt{\Pr s}y}+\frac{Gc\left(1-\lambda\right)}{s-a}+\frac{Gc\lambda e^{-\sqrt{\Pr s}y}}{s-a}\right\} \tag{6.1}$$

$$\frac{d^2\bar{\theta}}{dy^2}-\Pr\bar{\theta}=0 \tag{6.2}$$

$$\frac{d^2\bar{\phi}}{dy^2}-Scs\bar{\phi}=-Sr\Pr Sc\bar{\theta} \tag{6.3}$$

Laplace transformations of the initial and boundary conditions

$$y=0;\ \ \bar{u}=\frac{1}{s-a},\ \ \bar{\theta}=\frac{1}{s-a},\ \ \bar{\phi}=\frac{1}{s-a} \tag{6.4}$$

$$y\to\infty;\ \ \bar{u}\to 0,\ \ \bar{\theta}\to 0,\ \ \bar{\phi}\to 0 \tag{6.5}$$

(6.1)-(6.3) leads to

$$\bar{u}=\left\{\frac{1}{s-a}+\frac{Gr}{(s-a)(\Pr-1)(s-a_2)}+\frac{Gc(1-\lambda)}{(s-a)(Sc-1)(s-a_3)}+\frac{Gc\lambda}{(s-a)(Sc-1)(s-a_2)}\right\}e^{-\sqrt{a_1+s}y}$$

$$-\frac{Gr}{(s-a)(\Pr-1)(s-a_2)}e^{-\sqrt{\Pr s}y}-\frac{Gc(1-\lambda)}{(s-a)(Sc-1)(s-a_3)}e^{-\sqrt{Scs}y}-\frac{Gc\lambda}{(s-a)(\Pr-1)(s-a_2)}e^{-\sqrt{\Pr s}y} \tag{7.1}$$

$$\bar{\theta}=\frac{1}{s-a}e^{-\sqrt{\Pr s}y} \tag{7.2}$$

$$\bar{\phi}=\frac{1-\lambda}{s-a}e^{-\sqrt{Scs}y}+\frac{\lambda}{s-a}e^{-\sqrt{\Pr s}y} \tag{7.3}$$

Now taking inverse Laplace transformations on (7.1) - (7.3) we get

$$u=\begin{cases}u_{11}+u_{12}+u_{13}+u_{14}:\Pr\neq 1, Sc\neq 1\\ u_{21}+u_{22}+u_{23}+u_{24}:\Pr=1, Sc\neq 1\\ u_{31}+u_{32}+u_{33}+u_{34}:\Pr\neq 1, Sc=1\\ u_{41}+u_{42}+u_{43}+u_{44}:\Pr=1, Sc=1\end{cases} \tag{8.1}$$

$$\theta=\psi_1 \tag{8.2}$$

$$\phi = (1-\lambda)\psi_2 + \lambda\psi_1 \tag{8.3}$$

4. NUSSELT NUMBER

Nusselt number is given by

$$Nu = -\left(\frac{\partial\theta}{\partial y}\right)_{y=0}$$

$$= -Z_1 \tag{9.1}$$

5. SHERWOOD NUMBER

Sherwood number is given by

$$Sh = -\left(\frac{\partial\phi}{\partial y}\right)_{y=0}$$

$$= -\left\{(1-\lambda)Z_2 + \lambda Z_1\right\} \tag{9.2}$$

6. RESULTS AND DISCUSSION

Numerical calculations for velocity, temperature, concentration profiles, skin friction, Nusselt number, and Sherwood number at the plate are carried out to gain physical insight into the problem by assigning arbitrary chosen values to physical parameters such as time, thermal Grashof number, Accelerating parameter, Prandtl number, Permeability parameter, Magnetic parameter, Schmidt number, Mass Grashof number and Soret number.

In Figures 1-9 exhibit the variation of the velocity versus normal co-ordinate y under the influence of time, thermal Grashof number, Accelerating parameter, Prandtl number and Permeability parameter, Magnetic parameter, Schmidt number, Mass Grashof number and Soret number respectively. Figures 1-5 show that as increases the parameters time, thermal Grashof number, accelerating parameter, Prandtl number, and Permeability parameter, the fluid velocity increases. In other words, the fluid velocity at the plate decreases with high thermal diffusivity. In Figure 6 represents the velocity falls through the increase magnetic parameter. Figure 7 shows velocity increases near the plate, then a reversal of this trend as Schmidt number rises. Further, in Figures 8 and 9 velocity decrease near the plate as Mass Grashof and Soret numbers rise, then a reversal of this trend.

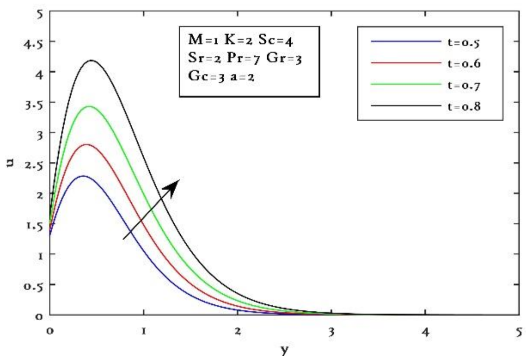

Figure 1: Velocity profile when t=0.5, 0.6, 0.7, 0.8

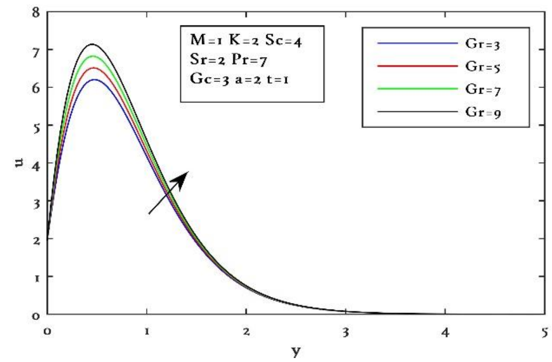

Figure 2: Velocity profile when Gr=3, 5, 7, 9

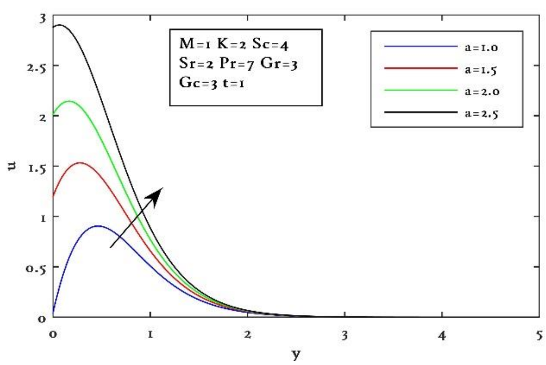

Figure 3: Velocity profile when a=1, 1.5, 2, 2.5

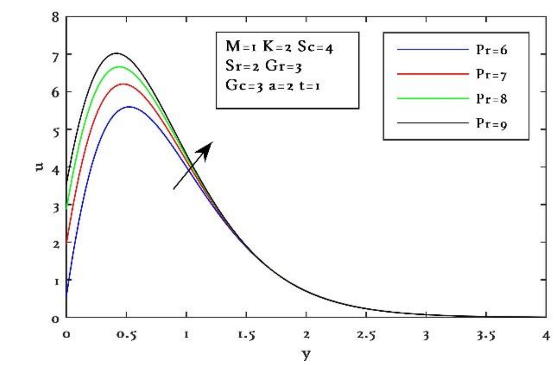

Figure 4: Velocity profile when Pr=6, 7, 8, 9

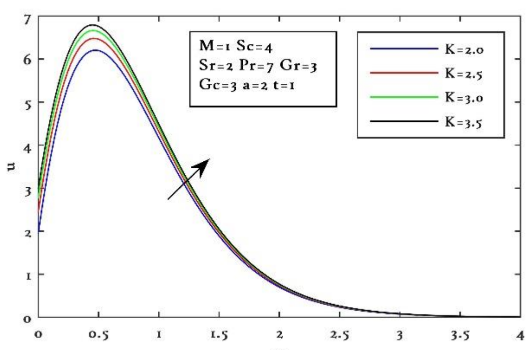

Figure 5: Velocity profile when K=2, 2.5, 3, 3.5

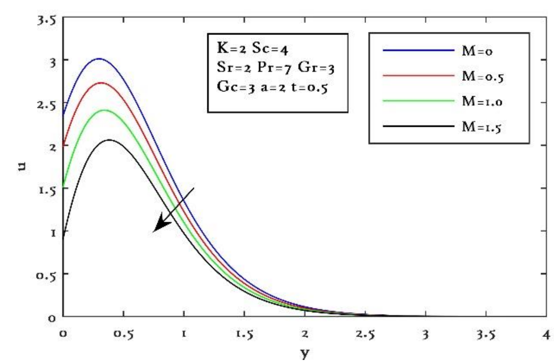

Figure 6: Velocity profile when M=0, 0.5, 1, 1.5

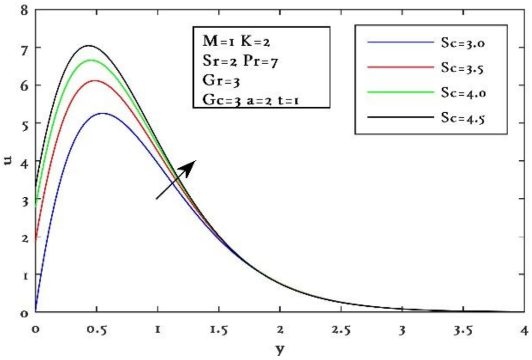

Figure 7: Velocity profile when Sc=3, 3.5, 4, 4.5

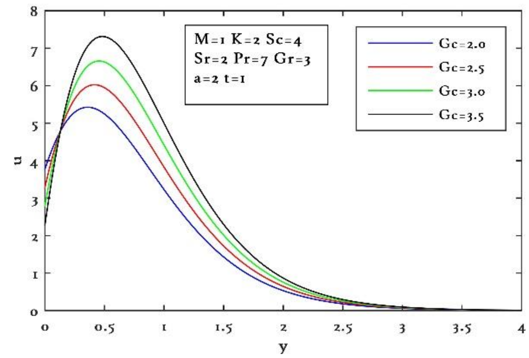

Figure 8: Velocity profile when Gc=2, 2.5, 3, 3.5

The effect of Prandtl number, time and accelerating parameter on temperature profile are presented in Figures 10-12. As of Figure 10 it is establish that the fluid temperature falls as Prandtl number increases. From Figures 11 and 12 the temperature is discovered to growth with raise in time duration and accelerating parameter of the plate. Figures 13-17 show how concentration profile changes with different values of the flow parameters such as Schmidt number, Prandtl number, Soret number, time and accelerating parameter respectively. We can see the concentration rises as the Schmidt number, Prandtl number, Soret number, time, and accelerating parameter increase. Concentration decreases for high mass diffusivity and high thermal diffusivity, as shown in Figures 13 and 14.

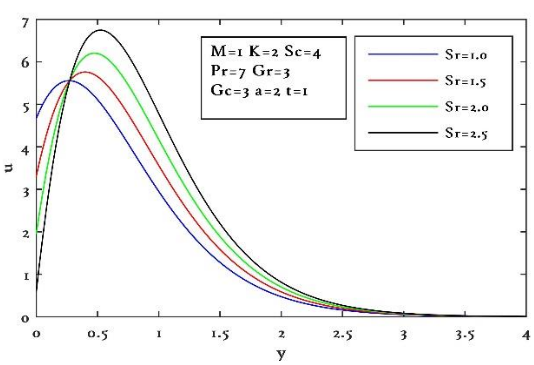

Figure 9: Velocity profile when Sr=1, 1.5, 2, 2.5

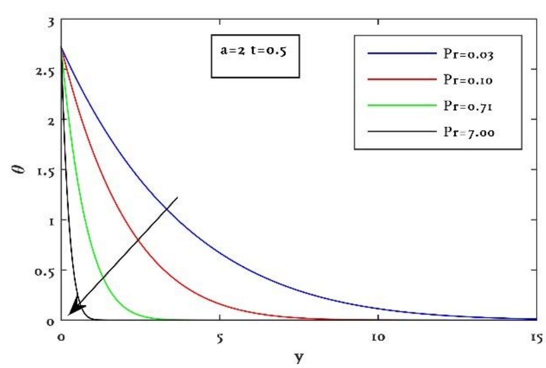

Figure 10: Temperature profile when Pr=.3, .1, .71, 7

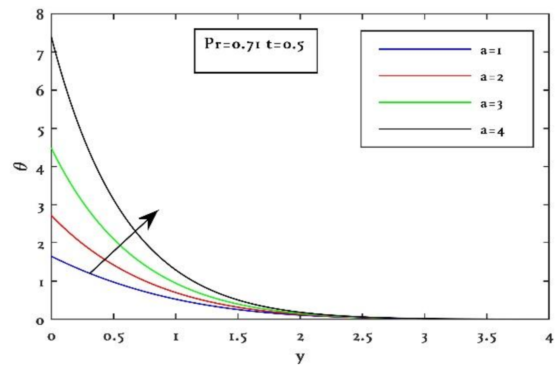

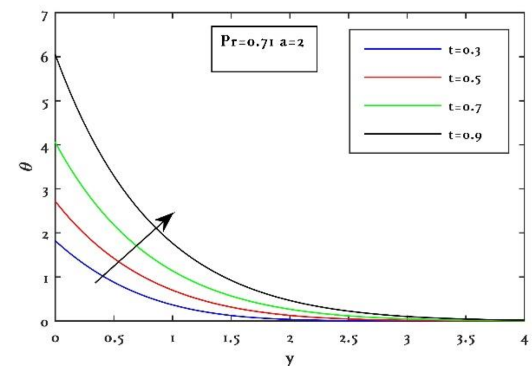

Figure 11: Temperature profile when a=1, 2, 3, 4 Figure 12: Temperature profile when t=.3, .5, .7, .9

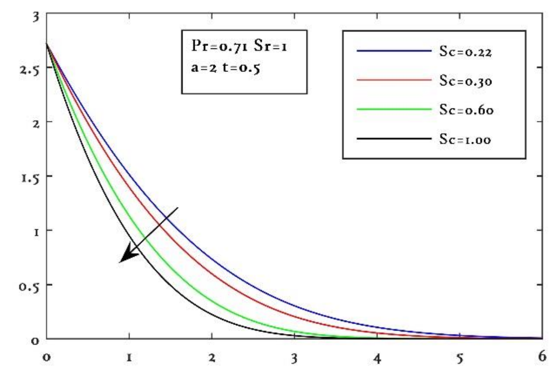

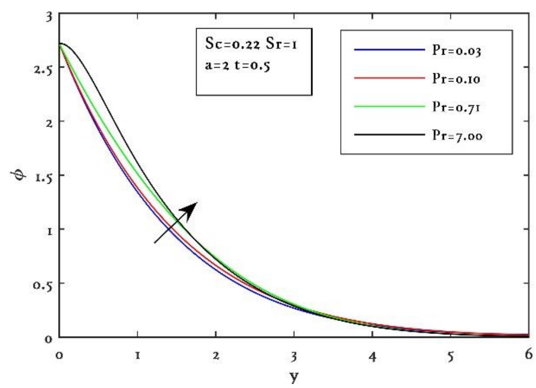

Figure 13: Concentration profile when Sc=.22, .3, .6, 1 Figure 14: Concentration profile when Pr=.03, .1, .71, 7

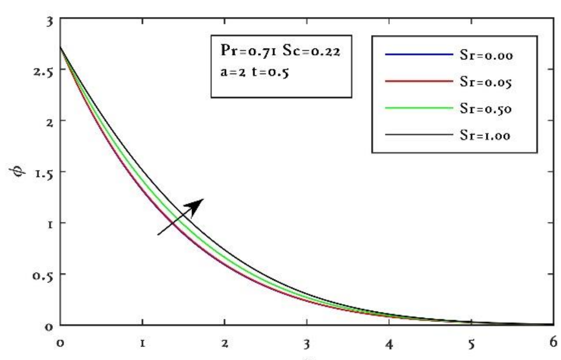

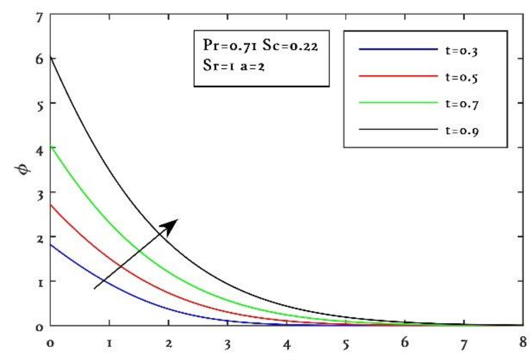

Figure 15: Concentration profile when Sr=0, 0.0 5, 0.5, 1 Figure 16: Concentration profile when t=.3, .5, .7, . 9

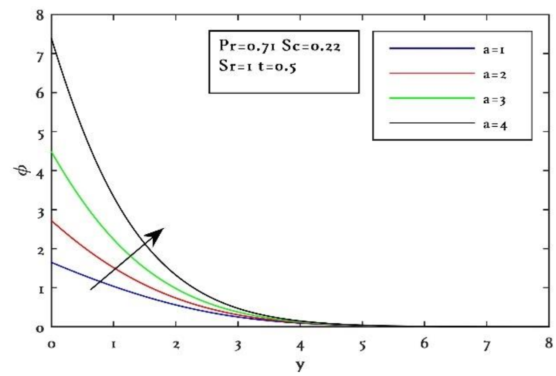

Figure 17: Concentration profile when a=1, 2, 3, 4

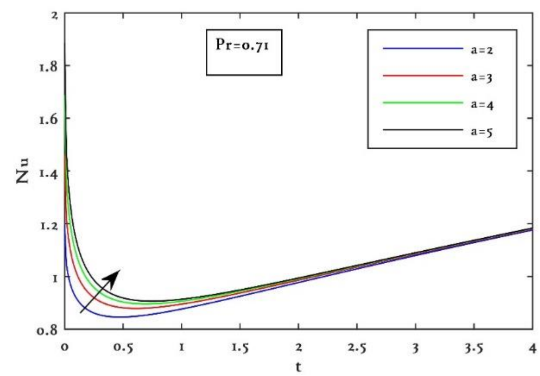

Figure 18: Nusselt number vs t when a=2, 3, 4, 5

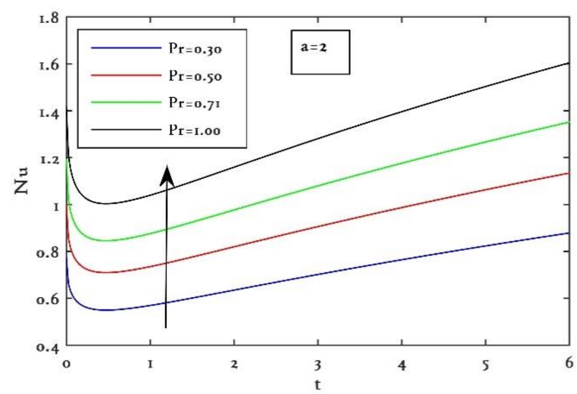

Figure 19: Nusselt number vs t when Pr=0.3, 0.5, 0.7, 1

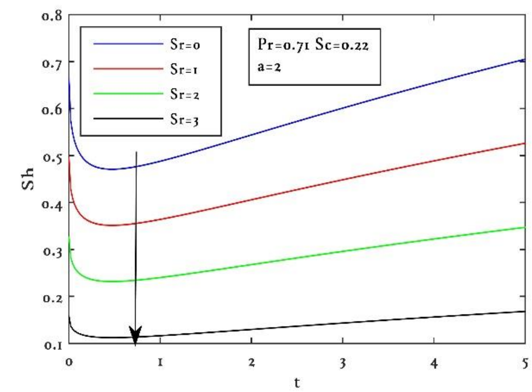

Figure 20: Sherwood number vs t when Sr=0, 1, 2, 3

Figures 18 and 19 denote the Nusselt number versus t for distinct ideals of accelerating limitation and Prandtl number. The Nusselt number from the figures rise with increment in accelerating parameter and Prandtl number of the plate. It is also found that the rate of heat transfer of the fluid falls for high thermal diffusivity. From Figures 20 and 21, it is observed that the Sherwood number against t fall under the effect of Soret number and Prandtl number. Figures 22 and 23 indicate that when the accelerating parameter and Schmidt number both increased, the Sherwood number increases significantly. On the other hand, rate of mass transfer at the plate falls for high mass diffusivity.

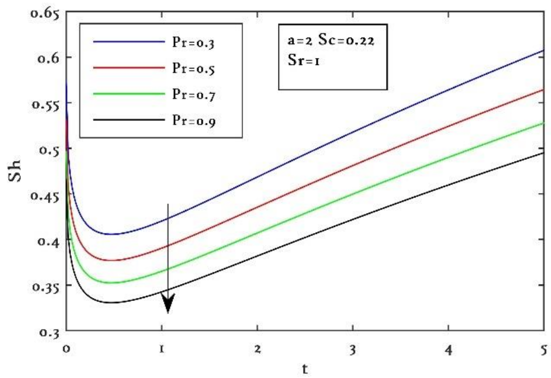

Figure 21: Sherwood number vs t when Pr=0.3, 0.5, 0.7,0. 9

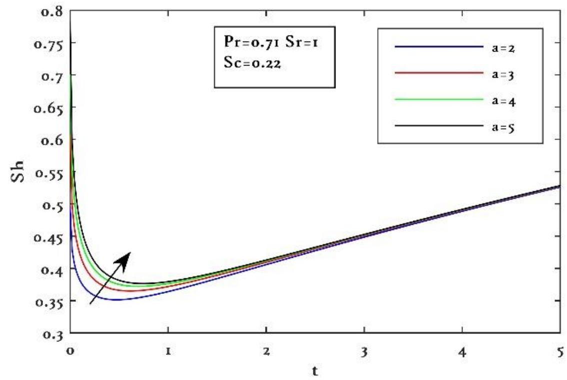

Figure 22: Sherwood number vs t when a=2, 3, 4, 5

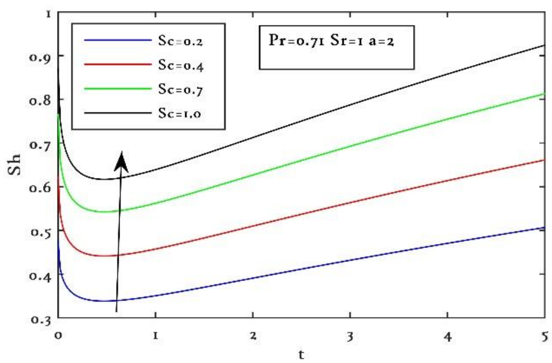

Figure 23: Sherwood number vs t when Sc=0.2, 0.4, 0.7, 1

7. CONCLUSION

- The velocity increase through an expansion in thermal Grashof number, Prandtl number and Permeability parameter.
- Velocity, temperature and concentration raise with an increase in time and accelerating parameter.
- The concentration and velocity fall with high thermal diffusivity.

APPENDIX

$$\lambda=-\frac{Sr\,\mathrm{Pr}\,Sc}{\mathrm{Pr}-Sc},\quad a_1=M+\frac{1}{K},\quad a_2=\frac{a_1}{\mathrm{Pr}-1},\quad a_3=\frac{a_1}{Sc-1},$$

$$\psi_1=\Psi(\mathrm{Pr},0,a,y,t),\quad \psi_2=\Psi(Sc,0,a,y,t),\quad \psi_3=\Psi(\mathrm{Pr},0,a_2,y,t),\quad \psi_4=\Psi(Sc,0,a_3,y,t),$$

$$h_1=e^{at}h(a_1+a,y,t),\quad h_2=e^{at}h(a_1+a_2,y,t),\quad h_3=e^{at}h(a_1+a_3,y,t),\quad Z_1=Z(\mathrm{Pr},0,a,t),$$

$$Z_2=Z(Sc,0,a,t),\quad u_{11}=h_1+\frac{A_1Gr}{\mathrm{Pr}-1}(h_1-h_2)+\frac{A_2Gc(1-\lambda)}{Sc-1}(h_1-h_3)+\frac{A_2Gc\lambda}{\mathrm{Pr}-1}(h_1-h_2),$$

$$u_{12}=-\frac{A_1Gr}{\mathrm{Pr}-1}(\psi_1-\psi_3),\quad u_{13}=-\frac{A_2Gc(1-\lambda)}{Sc-1}(\psi_2-\psi_4),\quad u_{14}=-\frac{A_1Gc\lambda}{\mathrm{Pr}-1}(\psi_1-\psi_3),$$

$$u_{21}=h_1-\frac{Gr}{a_1}h_1+\frac{A_2Gc(1-\lambda)}{Sc-1}(h_1-h_3)-\frac{Gc\lambda}{a_1}h_1,\quad u_{22}=\frac{Gr}{a_1}\psi_1,\quad u_{23}=u_{13},\quad u_{24}=\frac{Gc\lambda}{a_1}\psi_1,$$

$$u_{31}=h_1+\frac{A_1Gr}{\mathrm{Pr}-1}(h_1-h_2)-\frac{Gc(1-\lambda)}{a_1}h_1+\frac{A_1Gc\lambda}{\mathrm{Pr}-1}(h_1-h_2),\quad u_{32}=u_{12},\quad u_{33}=\frac{Gc(1-\lambda)}{a_1}\psi_2,$$

$$u_{34}=u_{14},\quad u_{41}=h_1-\frac{Gr}{a_1}h_1-\frac{Gc(1-\lambda)}{a_1}h_1+\frac{A_2Gc(1-\lambda)}{Sc-1}(h_1-h_3),\quad u_{42}=u_{22},\quad u_{43}=u_{33},\ u_{44}=u_{24},$$

$$\Psi(\xi,\eta,\zeta,y,t)=e^{\zeta t}\psi(\xi,\eta+\zeta,y,t),$$

$$\psi(\xi,\eta,y,t)=\frac{1}{2}\left[e^{\sqrt{\xi\eta}y}erfc\left(\frac{\sqrt{\xi}y}{2\sqrt{t}}+\sqrt{\eta t}\right)+e^{-\sqrt{\xi\eta}y}erfc\left(\frac{\sqrt{\xi}y}{2\sqrt{t}}-\sqrt{\eta t}\right)\right],$$

$$h(\eta,y,t)=\frac{1}{2}\left[e^{\sqrt{\eta}y}erfc\left(\frac{y}{2\sqrt{t}}+\sqrt{\eta t}\right)+e^{-\sqrt{\eta}y}erfc\left(\frac{y}{2\sqrt{t}}-\sqrt{\eta t}\right)\right],$$

$$Z(\xi,\eta,\zeta,t)=e^{\zeta t}\Omega(\xi,\eta+\zeta,t),\quad \Omega(\xi,\eta,t)=-\left[\sqrt{\frac{\xi}{\pi t}}e^{-\eta t}+\sqrt{\xi\eta}\,erf\left(\sqrt{\eta t}\right)\right].$$

NOMENCLATURE

List of symbols

$\vec{q}$: Fluid velocity

$\vec{B}$: Magnetic induction vector

$\vec{J}$: The current density

p : Fluid pressure

B_0 : Strength of uniform magnetic field

t : time

a : Accelerating parameter

v_0 : Suction velocity

C_p : Specific heat at constant pressure

M : Hartmann number or magnetic parameter

Pr : Prandtl number

Sc : Schmidt number

E : Eckert number

Sr : Soret number

Gr: Thermal Grashof number

Gc: Mass Grashof number

T : Fluid temperature

T_m : Mean fluid temperature

T_w : Wall temperature

T_∞ : Fluid temperature far away from the plate

K_T : Thermal diffusion ratio

D_M : Mass diffusivity

C : Species concentration

C_w : Wall concentration

C_∞ : Concentration far away from the plate

u_0 : Velocity of the plate

Greek symbols

ρ : Fluid density

ν : Kinematic viscosity

σ : Electrical conductivity

κ : Thermal conductivity

μ : Co-efficient of viscosity

β : Volumetric coefficient of thermal expansion

β_c : Volumetric coefficient of thermal expansion with concentration

θ : Dimensionless temperature

ϕ : Dimensionless concentration

CONFLICT OF INTERESTS

The author(s) declare that there is no conflict of interests.

REFERENCES

[1] H. Alfven, Existence of electromagnetic-hydrodynamics waves, Nature, 150 (1942), 405-406.

[2] J.A. Shercliff, A text of magnetohydrodynamics, Pergamon, New York, (1957).

[3] V.C.A. Ferraro and C. Plumpton, An introduction to magneto-fluid mechanics, Clarendon Press, Oxford, (1966).

[4] K.R. Cramer and S.I. Pai, Magnetofluid dynamics for engineers and applied physicists, McGraw-Hill, New York,

USA, (1973).

[5] D.A. Nield and A. Bejan, Convection in porous media, 2nd Edition, Springer Verlag, Berlin, (1998).

[6] P.S. Hiremath and P.M. Patil, Free convection effects on oscillatory flow of couple stress field through a porous medium, Acta Mech. 98(1993), 143-158.

[7] S.R. Rao, G. Vidyasagar and G.V.S.R. Deekshitulu, Unsteady MHD free convection Casson fluid flow past an exponentially accelerated infinite vertical porous plate through porous medium in the presence of radiation absorption with heat generation/absorption. Mater. Today: Proc. 42(2021), 1608-1616.

[8] R. Mahato and M. Das, Effect of suction/blowing on heat-absorbing unsteady radiative Casson fluid past a semi-infinite flat plate with conjugate heating and inclined magnetic field, Pramana 94 (2020), 127.

[9] E. Omamoke, E. Amos and K.W. Bunonyo, Radiation and heat source effects on MHD free convection flow over an inclined porous plate in the presence of viscous dissipation, Amer. J. Appl. Math. 8 (2020), 190-206.

[10] S. Lavanya, B. Devika and D.C. Kesavaiah, Radiation effect on unsteady free convective MHD flow of a viscoelastic fluid past a tilted porous plate with heat source, J. Xidian Univ. 14 (2020), 2298- 2312.

[11] E. Omamoke and E. Amos, Chemical Reaction, radiation and heat source effects on unsteady MHD blood flow over a horizontal porous surface in the presence of an inclined magnetic field, Int. J. Sci. Eng. Res. 11 (2020), 1187-1192.

[12] A. Orhan and K. Ahmet, Radiation effect on MHD mixed convection flow about a permeable vertical plate, Heat Mass Transfer, 45 (2008), 239-246.

[13] N. Sandeep, Radiation and inclined magnetic field effects on unsteady hydromagnetic free convection flow past an impulsively moving vertical plate in a porous medium, J. Appl. Fluid Mech. 7(2014), 275-286.

[14] B.K. Sharma, R.C. Chaudhary and P.K. Sharma, Fluctuating mass transfer on three-dimensional flow through a porous medium with variable permeability, Adv. Theor. Appl. Math. 2(2007), 257–267.

[15] J.R. Pattnaik, G.C. Dash and S. Singh, Radiation and mass transfer effects on MHD free convection flow through porous medium past an exponentially accelerated vertical plate with variable temperature, Ann. Faculty Eng. Hunedoara 10(2012),175.

[16] A. Selvaraj and E. Jothi, Heat source impact on HMD and radiation absorption fluid flow past an exponentially accelerated vertical plate with exponentially variable temperature and mass diffusion through a porous medium, Mater.

Today: Proc. (2021), https://doi.org/10.1016/j.matpr.2020.11.919.

[17] V. Rajesh and S.V.K. Varma, Heat source effects on MHD flow past an exponentially accelerated vertical plate with variable temperature through porous medium, Appl. Math. Mech. 6(12) (2010), 68-78.

[18] G.S. Seth, M.S. Ansari and R. Nandkeolyar, MHD natural convection flow with radiative heat transfer past an impulsively moving plate with ramped wall temperature, Heat Mass Transfer, 47(5) (2011), 551-561.

[19] R.S. Raju, K. Sudhakar, M. Rangamma, The effects of thermal radiation and heat absorption on an unsteady MHD free convection flow past an infinite vertical plate with thermal diffusion and diffusion thermo, J. Inst. Eng.: Ser. C, 94(2013), 175–186.

[20] N. Ahmed, Soret and radiation effect on transient MHD force convection from an impulsively started infinite vertical plate, J. Heat Transfer 134 (2012), 062701.

[21] N. Ahmed and S. Sengupta, Thermo-diffusion and diffusion-thermo effects on a three-dimensional MHD mixed convection flow past an infinite vertical porous plate with thermal radiation, J. Magnetohydrodynamics, 47 (2011), 41-60.

[22] N. Ahmed, MHD convection with Soret and Dufour effects in a three-dimensional flow past an infinite vertical porous plate, Can. J. Phys. 88 (2010), 663-674.